Radio Science

RESEARCH ARTICLE
10.1029/2021RS007336

Deriving Ionospheric Total Electron Content by VLBI Global Observing System Data Analysis During the CONT17 Campaign

Sanam Motlaghzadeh[1,2], M. Mahdi Alizadeh[1,3], Roger Cappallo[4], Robert Heinkelmann[3], and Harald Schuh[3,5]

[1]Faculty of Geodesy and Geomatics Engineering, K. N. Toosi University of Technology, Tehran, Iran, [2]Faculty of Science, University of Helsinki, Helsinki, Finland, [3]German Research Centre for Geosciences (GFZ), Potsdam, Germany, [4]MIT Haystack Observatory, Westford, MA, USA, [5]Institute of Geodesy and Geoinformation Sciences, Technical University of Berlin, Berlin, Germany

Key Points:

- We studied the variation of ionospheric total electron content over six sites as determined using data of the new geodetic *very* long baseline interferometry (VLBI) system, VLBI global observing system (VGOS), in December 2017
- By enhancing the model, we estimated the temporal variation of the latitudinal ionosphere gradient and achieved more accurate results
- We compared our results with global navigation satellite system vertical total electron content which enabled us to detect an error in the sign of the VGOS differential total electron content calculation

Correspondence to:

S. Motlaghzadeh,
ghodsiyehmotlaghzadeh@helsinki.fi

Citation:

Motlaghzadeh, S., Alizadeh, M. M., Cappallo, R., Heinkelmann, R., & Schuh, H. (2022). Deriving ionospheric total electron content by VLBI global observing system data analysis during the CONT17 campaign. *Radio Science*, *57*, e2021RS007336. https://doi.org/10.1029/2021RS007336

Received 13 JUL 2021
Accepted 11 SEP 2022

Author Contributions:

Conceptualization: M. Mahdi Alizadeh
Data curation: Sanam Motlaghzadeh, Roger Cappallo
Formal analysis: Sanam Motlaghzadeh
Investigation: Sanam Motlaghzadeh
Methodology: Sanam Motlaghzadeh
Resources: Roger Cappallo
Software: Sanam Motlaghzadeh
Supervision: M. Mahdi Alizadeh, Roger Cappallo
Validation: M. Mahdi Alizadeh, Roger Cappallo
Writing – original draft: Sanam Motlaghzadeh

Abstract This article focuses on the new generation of geodetic very long baseline interferometry (VLBI), the VLBI global observing system (VGOS), and measurements carried out during the CONT17 campaign. It uses broadband technology that increases both the number and precision of observations. These characteristics make VGOS a suitable tool for studying the atmosphere. This study focuses on the effects of the ionosphere on VGOS signals using a model that incorporates and extends ideas originally published in Hobiger et al. (2006, https://doi.org/10.1029/2005RS003297). Our investigation revealed that the differential total electron content (dTEC) data product calculated with the VGOS post-processing software had a sign error that fortunately, does not change the final values of the phase and group delay. Therefore, this study was a way to identify this problem within the dTEC product. After diagnosing and solving this problem, the underlying model was modified such that instead of considering a single unknown for the latitude gradient of the ionosphere, a time series of latitude gradients were considered that enhanced the resulting vertical total electron content (VTEC) estimates. For evaluation purposes, time series of VTEC at each station during the CONT17 campaign were compared with VTEC obtained from the global navigation satellite system (GNSS). The final agreement between VGOS and GNSS was between 1.1 and 5.9 TEC units (TECU).

Plain Language Summary The ionosphere is the upper layer of the atmosphere, where free ions and electrons bend and delay the extragalactic radio waves, which are received at ground stations. Such radio waves can be exploited for positioning or detection of Earth's crustal movements; thus, detecting the ionospheric effect on these signals is of paramount importance. This paper investigates the effects of this medium on the signals emitted from celestial bodies called "quasars" and received by a system called VLBI global observing system (VGOS) which is a new generation of very long baseline interferometry (VLBI). Being inspired by Hobiger et al. (2006, https://doi.org/10.1029/2005RS003297), we used a station-dependent model to estimate the temporal variation of the ionospheric total electron content (TEC). Our initial results allowed us to correct an unreported error in the software package of VGOS, during the CONT17 campaign which we analyzed. We also enhanced the station-dependent model so that it could achieve a better estimation of TEC.

1. Introduction

The design of the VLBI global observing system (VGOS) addresses many deficiencies of its legacy system, very long baseline interferometry (VLBI): it has small antennas that can slew between sources quickly and allow faster sampling for better coverage of the ever-changing atmosphere, the broadband technology that increases the sensitivity and the delay precision, and an instantaneous data recording system with a rate of 16 Gbps (1 Gbps = 1,000 bits per second) that enables data acquisition from weaker sources (up to 250 mJy, where 1 Jy = 10^{-26}Wm^{-2} Hz^{-1}) and prevents the antennas from overheating (Petrachenko et al., 2009). The broadband characteristic of VGOS and how the broadband delay is obtained allows the ionosphere contributions to be estimated more accurately. Instead of using the S and X bands of geodetic VLBI systems, the broadband technology uses a range of frequencies (2–14 GHz). Coherently combining the data from these four bands and two polarizations, allows the delay precision of single observations to be better than 16 ps (1 ps = 10^{-12} s) (Niell et al., 2018). Using this

Writing – review & editing: M. Mahdi Alizadeh, Roger Cappallo, Robert Heinkelmann, Harald Schuh

system, the baseline length estimates can be as precise as 0.3 mm. For a more detailed description of the VGOS system and its contribution to geodetic VLBI, see Niell et al. (2018).

The focal point of this paper lies in an updated way to calculate ionospheric parameters. In legacy S/X VLBI systems utilizing X- and S-band, the differential delay caused by the ionosphere is removed by forming a linear combination of the S and X band group delays. This procedure is done after the correlation stage. Instead, in the VGOS data pipeline, estimates of differential total electron content (dTEC) for each baseline are made during the correlation post-processing (Cappallo, 2015). Niell et al. (2018) showed consistency between VGOS dTEC and the differenced TEC obtained by global navigation satellite systems (GNSS) data. For legacy S/X systems Hobiger et al. (2006) came up with a station-dependent model for estimating the frequency-dependent delay caused by the ionosphere and thus extracting the time series of vertical total electron content (VTEC) for each of the stations. To avoid repetition, throughout the paper, we mention this model by "the station-dependent model." The method described in this paper is inspired by the station-dependent model because it's not dependent on any external data other than VLBI, but still estimates the variation of the VTEC parameter during the observing session. Since VGOS is a new system and is in a number of ways more complex than the legacy S/X systems, subtleties are arising from phase calibration and dTEC estimation that had to be taken into account in our analysis. Moreover, the original station-dependent model considered only one unknown parameter for the latitude gradient of the ionosphere. In this study, however, this assumption is enhanced by introducing a time series for ionosphere latitude gradient. Another difference is that we used dTEC as the input data to estimate VTEC above each station point, whereas, in the original station-dependent model, the ionospheric delay was used for this purpose.

To evaluate our result initially, the final VTEC time series are compared with VTEC from GNSS observations. GNSS includes different satellite missions aim at positioning; namely, global positioning system (GPS), Galileo, Global'naya NAvigatsionnaya Sputnikovaya Sistema (GLONASS), and BeiDou. Using a dual frequency GNSS receiver, one can form combinations between observations and estimate the ionospheric contribution, as it explained for example, in Hofmann-Wellenhof et al. (2001). A similar practice has been attempted with the legacy VLBI system. In Dettmering et al. (2011), the VTEC derived from geodetic VLBI is compared to the VTEC derived from other methods, including GNSS and the GNSS VTEC is consistent with VLBI VTEC. In this work it is shown that the GNSS estimates have higher values than VLBI estimates, which agrees with our results. In Sekido et al. (2003) the VTEC values derived from geodetic VLBI have been compared with global ionospheric map (GIM) from center of orbit determination in Europe (CODE), which is obtained from GNSS data, and showed that there is a 90% correlation between the two data sets for the short-length baselines. Moreover, Hobiger et al. (2006) has also made the same comparison with GIM for all VLBI sessions from 1995 to 2006 and concluded that the overall mean difference between the two methods is −2.8 TECU which shows a good agreement. He also has shown that GNSS-based VTEC is slightly higher than VLBI TEC, which matches our results.

2. Method

2.1. Extraction and Modeling of the Ionospheric Parameters

Interferometric systems such as S/X VLBI or VGOS are used to observe the difference in the interferometric phase of a noise signal from an extragalactic radio source, as received at two different antennas. The principal geodetic observable is group delay and according to Cappallo (2015), the correlation between group delay and dTEC is high (more than 90%). Therefore, the precision and wide frequency coverage of the VGOS observations necessitate accounting for the ionospheric effect at the post-correlation analysis stage. For VGOS, determining this dTEC parameter is performed by the *fourfit* program, which is distributed with the software package Haystack observatory processing software (HOPS). The phase model used in this program is (Cappallo, 2016):

$$\Phi(f) = \tau_g * (f - f_0) + \Phi_0 - \frac{1.3445 * \mathrm{dTEC}}{f} \tag{1}$$

where Φ is the interferometric phase (rotation), τ_g is the group delay (ns), f is the frequency (GHz), f_0 is the fourfit reference frequency (GHz), Φ_0 is the phase (rotation) at f_0, and dTEC is the differential TEC (TECU = $\frac{10^{16}}{m^2}$). Among other parameters, for each observation, a value for τ_g and dTEC is estimated; this study uses those estimates of dTEC as our raw observable. Since our raw data come from the output of the fourfit program, it is useful to study in-depth how dTEC is retrieved.

The model used by the correlator has imperfectly known physical parameters, such as source and station coordinates, station clock, and a non-hydrostatic part of the troposphere delay zenith wet delay. The estimates of each parameter contain errors and thus increase the total error. As a result, there are non-zero residual delays and delay-rates. *Fringe-fitting* is a post-correlation process that is responsible for correcting the errors of the estimates (e.g., Cotton, 1995). Based on Equation 1, the parameter values (dTEC and the group delay) are adjusted within fourfit, in a manner such that all of the channel phases are as similar as possible, resulting in the greatest coherent sum of the individual channel phasors (Cappallo et al., 2017).

Assuming small errors in the a priori parameters, the change in phase (to first order) can be written:

$$\Delta\Phi(t, f) = \Phi_0 + \left(\frac{\partial\Phi}{\partial f}\Delta f\right) + \left(\frac{\partial\Phi}{\partial t}\Delta t\right) \tag{2}$$

where $\frac{\partial\Phi}{\partial f}$ is the residual group delay and $\frac{\partial\Phi}{\partial t}$ is the residual fringe rate. Equation 2 is also called the resolution function, which is to be maximized by finding the optimal group delay and fringe rate (Rogers, 1970). The optimal delay and fringe rate are found through a search of coherently summed amplitudes, over a 3-dimensional grid with axes denoting single-band delay (the group delay within each frequency channel), multi-band delay (the group delay after tying together the phases across all frequency channels), and group delay-fringe rate (simply delay-rate) (see, e.g., Cotton, 1995). VGOS fringe fitting for an experiment requires multiple setup runs of the program fourfit under different configurations, to correct channel phase offsets and find delay offsets for the bands (Barrett et al., 2019). Within each scan, polarizations are coherently combined, and a fit is performed, yielding a set of calibrated broadband VGOS observables. The independent parameters that are estimated are interferometer phase, group delay, group delay-fringe rate, and dTEC (see Equation 1) and they are adjusted such that the coherently summed (over all channels) complex fringe amplitude is at a maximum.

Ideally, the phase calibration tones would allow the automatic adjustment of channel phases to achieve maximum coherence. In practice, though, particularly during the early period of VGOS due to the presence of hardware problems, it is necessary to make some "manual" adjustments to the channel phases. During the so-called manual phase calibration, the correlator engineer picks several strong scans and determines channel-by-channel phase offsets to maximize the fringes. Unfortunately, this has been shown to introduce small frequency-independent phase signatures, which mimic the effect of ionospheric dispersion. In essence, each station has a small, unknown, yet constant TEC value added to every observation. This makes it necessary to estimate and remove the effect of this *dispersion offset*, as done in this research.

As shown in Equation 1, the phase contribution (in radians) due to the ionosphere is:

$$\Delta\Phi = -1.3445 * \left(\frac{\mathrm{dTEC}}{f}\right) \tag{3}$$

where dTEC is the difference of TEC (in TECU) above the two stations and the phase offset is applied to each individual frequency channel (Cappallo et al., 2017). The method used in fourfit to determine dTEC is to successively estimate the other independent parameters (phase, delay, and delay rate) at a grid of fixed values of dTEC that span a specified range. For each trial value of dTEC, a complete fringe fit is performed and from these fits, the interpolated maximum is found. The chosen value of dTEC (at the optimal value of delay and rate) maximizes the coherent sum of complex cross-spectral power. Note that for VGOS the cross-power spectra from the correlator need to be combined prior to the fringe-fit. Due to the use of linearly polarized feeds, there are four complex correlation products (XX, YY, XY, YX), which are co-added into a Stokes Intensity equivalent, taking into account the parallactic angles of the antenna feeds (Cappallo, 2016).

2.2. Formulation of the Theoretical Model

The ionosphere is a dispersive medium where signals are both refracted and delayed in a frequency-dependent manner (Böhm and Schuh, 2013). In the current study, we ignore ionospheric refraction, as well as the higher-order terms of ionospheric delay (Hawarey et al., 2005), as they are currently below our sensitivity level.

The differential ionosphere can be treated as the difference of the TEC along the two slanted ray paths, STEC_i

$$\mathrm{dTEC} = \mathrm{STEC}_2 - \mathrm{STEC}_1 \tag{4}$$

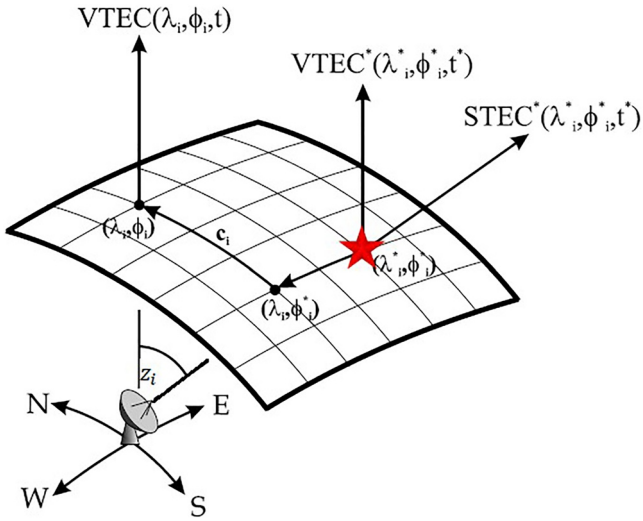

Figure 1. Vertical total electron content (VTEC) at the ionospheric pierce point and its relation to the VTEC on the station point (taken from Hobiger et al. [2006]).

Figure 1 illustrates the single layer model (SLM) for the ionosphere (Schaer, 1999). According to this assumption, no variation in longitude is explicitly solved for—changes in longitude only enter implicitly through the time dependency of parameters (Dettmering et al., 2011).

The discrepancy between our work and the original station-dependent model arises from the fact that the original station-dependent model uses the ionospheric delay ($\tau_X - \tau$, where τ_X is the total delay in X band and τ is the ionospis the ionospe-free combination) dTEC using the ionospheric factor $\frac{40.3}{c*f}$ and converts it to dTEC using the ionospheric factor $\frac{40.3}{c.f}$ (where c is the speed of light and f is the frequency) to estimate the VTEC values, but our fundamental datum is dTEC data and there is no need to the converting factor. Moreover, we improved the model represented in the original station-dependent model in ways; namely by changing the definition of latitude gradient and producing a time series for it, using a different piece-wise linear function for generating time series, removing the non-negative constraint matrix for estimating VTEC, and substituting the instrumental delay with the dispersion offset (see section 2-1) as an unknown parameter.

In Figure 1 quantities with * superscript refer to the ionsopheric pierce point (IPP), the i index refers to the station and z_i is the zenith angle of the station. The longitude offset, $\lambda_i^* - \lambda_i$, is compensated for by changing the observation timetag, that is, $t_i\, t + \frac{\Delta\lambda_i}{15}$, $i = 1,2$, where λ is in degrees, t is in hour, and degrees and hour are related to each other by hour = degrees/15. The gradient of TEC in latitude, -g, is solved for, and multiplied by the latitude offset, $\phi_i^* - \phi_i$. Thus, the VTEC in IPP can be related to the VTEC in station with Equation 5.

$$\mathrm{VTEC}^* = \mathrm{VTEC} + \Delta\phi \cdot g \tag{5}$$

where VTEC* is the VTEC in IPP, VTEC is the VTEC at the station, and $\Delta\phi$ is the latitude difference between station and IPP. Based on Equation 4 and considering the additional effect that is produced during the correlation process, the observation equation now reads:

$$\mathrm{dTEC} = \left[F(z_2) * (\mathrm{VTEC}_2(t_2^*) + g_2(t_2^*) * \Delta\phi_2)\right] - \left[F(z_1) * (\mathrm{VTEC}_1(t_1^*) + g_1(t_1^*) * \Delta\phi_1)\right] + \delta_2 - \delta_1 \tag{6}$$

where VTEC_i is the piece-wise linear function for VTEC, $g_i(t)$ is the piece-wise linear latitude gradient function (in TECU/deg), δ_i is the dispersion offset, and F(z) is the mapping function. The dispersion offsets make the design matrix singular, as VLBI only makes differential delay measurements; hence to resolve them, similar to the original station-dependent model, the additional constraint is placed that the sum of all station dispersion offsets is equal to zero. Moreover, similar to the original station-dependent model, we adopted the modified SLM (MSLM) mapping function of the ionosphere (Schaer, 1999):

$$F(z) = \frac{1}{\sqrt{1 - \left(\frac{R_E}{R_E + H}\sin(\alpha z)\right)^2}} \tag{7}$$

where $\alpha = 0.9782$ is the scaling factor, and $H = 506.7$, R_E is the Earth radius, and z is the zenith angle. In this study, due to the high temporal resolution of VGOS observations which is one minute or less, each group of 15 sequential observations represents one interval, whereas in the original station-dependent model this value was set to 8.

Our model consists of three components: for each station, there is a time series representing VTEC above that station, another time series for the latitude gradient of VTEC, and a dispersion offset. When defining the time series in the station-dependent model, an offset is introduced and the slope between each two data points are estimated. This method increases the error, since by changing the offset value the whole time series will move up or down. Instead, we implement piece-wise linear polynomials that estimate only the values of endpoints, both for the VTEC and latitude gradient time series; the model estimates the values of the endpoints of each connected

segment. Specifically, if the endpoints are a set of $(n + 1)$ values having a time t_k and a rate p_k, with k running from 0 through n, when t lies in the interval $[t_k, t_{k+1}]$ the piece-wise linear function VTEC(t) is given by:

$$\mathrm{VTEC}(t) = \frac{(t_{k+1} - t) * p_k + (t - t_k) * p_{k+1}}{t_{k+1} - t_k} \tag{8}$$

To perform a Least-Squares fit, we need to form a residual vector and minimize the squared sum of these residuals weighted by a weight matrix. The weight matrix (P) is defined by w_k which is the weight of the mapping function divided by the error of observations (reported by the fourfit program).

$$P = \frac{w^j(z_1, z_2)}{\sigma^2} \tag{9}$$

where σ is the vector of observations error (here dTEC formal error) and w^j is $\left(\frac{1}{\sqrt{\frac{1}{2}[F(z_2)]^2 + \frac{1}{2}[F(z_1)]^2}}\right)^j$.

According to Hobiger and Schuh (2004), the best option for j is 4. If we define the Δx as unknowns, A as design matrix, ΔY as *observed minus calculated* vector, $v = A\Delta x - \Delta Y$ as residuals and P as the weight matrix (which is inversely proportional to the square of observations uncertainty), by minimizing $v^T P v$ the problem will be solved as seen in Equation 10. The derivatives with respect to Δx must be set to zero (Koch, 1997).

$$\min v^T P v = \min\left(\Delta x^T A^T P A \Delta x - 2A^T P \Delta Y \Delta x + \Delta Y^T P \Delta Y\right) \tag{10}$$

To ensure that the residual vector (v) is converging, and assess the goodness-of-fit of our calculated dTEC $A\Delta x$ to the observed dTEC ΔY, we used a reduced chi-square statistic or the variance of unit weight. If the statistic is bigger than 1, the estimation procedure stops. In Equation 11 one can find the statistics of reduced chi-square test.

$$\chi^2_{df} = \frac{\left(v^T P v\right)}{df} \tag{11}$$

where df is the degree of freedom (observations-unknowns). The estimations accuracy is stored in a variance-covariance matrix, Q:

$$Q = \left(A^T P A\right)^{-1} \tag{12}$$

The final standard deviation of estimates is found by multiplying Equation 11 to the diagonal elements of Q in Equation 11, that is, $\sigma_i = \sqrt{Q_{ii}\chi^2_{df}}$ (Koch, 1997).

We start the processing directly with dTEC that is found in the "Observables" folder of the data in the vgosDB file format (for more information about vgosDB format, see Gipson [2015]), alongside its formal error of about 0.04 TECU reported by the fourfit program. The analysis described above is performed using MATLAB.

3. Data and Processing

Vienna VLBI software (VieVS) was developed at the Vienna university of technology (TU Wien) using MATLAB software and has been used extensively for analyzing VLBI data. After processing each session, a mat-structure file is stored in which all scans are organized sequentially, from which VTEC above each station can be extracted (Böhm et al., 2018).

For this study, we initially used VieVS to process the VGOS sessions, acquired in the CONT17 campaign (see Behrend et al., 2020) and then, using the mat-structure file obtained by VieVS, applied the algorithm mentioned in section 2-2 for deriving VTEC and latitude gradient values from this data set. This campaign, carried out by IVS (International VLBI Service, see Nothnagel et al., 2017), took place over a time period of about two weeks that only about a third of which, 5 days from the interval 3–8 December 2017, were observed with a VGOS broadband network. Principally we used data from the 3 December session to construct TEC and its latitude gradient above each station, although other sessions were processed for comparison. The stations that participated in this campaign were the Goddard Geophysical and Astronomical Observatory (GGAO12M), Westford (WESTFORD), and Kokee (KOKEE12M) in the United States, Ishioka (ISHIOKA) in Japan, Yebes (RAEGYEB) in Spain, and

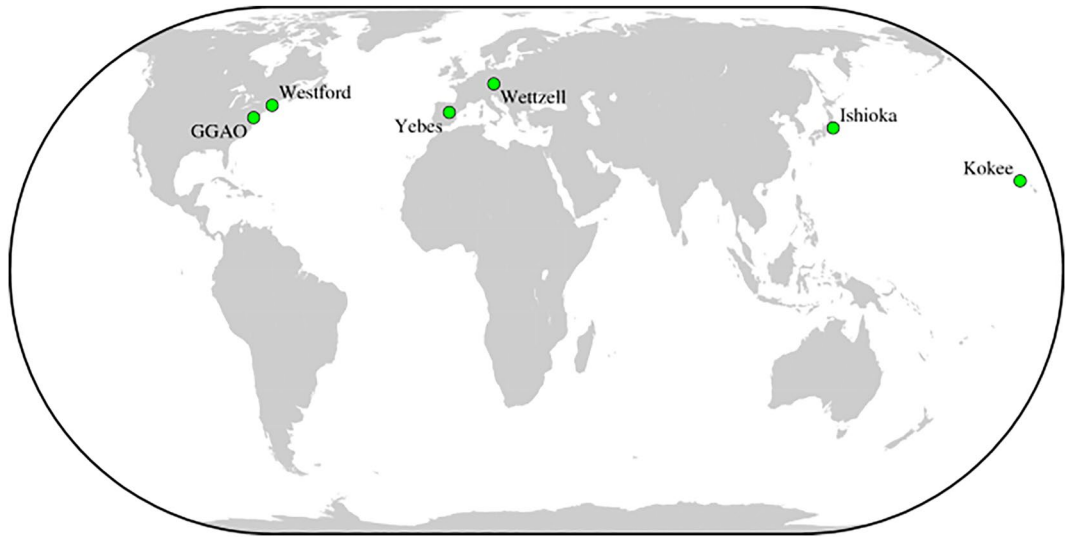

Figure 2. The green points depict the stations that participated in the CONT17 campaign (Behrend et al., 2020).

Wettzell (WETTZ13S) in Germany. Their geographical distribution can be seen in Figure 2. In this campaign, antennas and VGOS backends were used to observe in 4 bands, each of which consisted of 8 dual-polarization (linear X & Y) 32 MHz wide channels. In this campaign, the Haystack Observatory Post-processing Software (HOPS) was used to determine dTEC values.

4. Results and Discussion

Using the equations and methods outlined in Section 2.2, the VTEC and its latitudinal gradient time series above each of these six stations were estimated from dTEC data. To evaluate the estimated VTEC, we compared our results with the VTEC extracted from GNSS observations using Gopi software (Seemala, 2011). The observation files in the format of Receiver INdependent EXchange (RINEX) (Romero, 2020) for GGAO12M, ISHIOKA, KOKEE12M, RAEGYEB, and WETTZ13S were downloaded from international GNSS service (IGS) data center and imported to Gopi software, while the observation file for WESTFORD station was downloaded from University NAVstar COnsortium (UNAVCO) (Rocken et al., 1995). The output of Gopi software is the STEC values along with elevation angle values. Using this two information and the mapping function (Equation 7) the VTEC at the station point is calculated. The time interval of the GPS observation files is 30 s; therefore, we need a time interpolation to obtain the VTEC values at the same time as VGOS VTEC is estimated. The software also provides the user with a standard deviation of the STEC estimations, which is in range of (0.08 TECU, 8.14 TECU) and on average it is 1.6 TECU. Using the mapping function, the error in slant direction can be mapped to the vertical direction, which is in range of (0.02 TECU, 8.98 TECU) and on average it is 1.8 TECU. For more information on how to extract STEC from GNSS data read for example, Seemala and Valladares (2011).

To validate the latitude gradients results, the GIM from the CODE which is issued in standard IONosphere map EXchange (IONEX) format were used (see e.g., Roma-Dollase et al., 2018). The GIM is a global ionosphere map, providing VTEC from GNSS observations. These files provide global values of VTEC every 2 hr with the spatial resolution of 2.5° in latitude and 5° in longitude (Schaer et al., 1998). Interpolating the coordinates of the CONT17 VGOS stations and the IPP points, the latitude gradient time series above each station was calculated from the map data. The accuracy cited for the GIM data varies with position and time, but it is generally within ±2 to ±8 TECU, for land and ocean stations respectively (Oceanic sites have degraded accuracy due to the sparsity of sites. For more information, see http://www.igs.org/products/data).

Our first efforts at comparing VGOS results and GNSS data showed that the VTEC patterns tracked each other poorly. To find the source for this disagreement, we employed a closure constraint to assess the accuracy of dTEC. All the possible triangles of baselines were considered to check that the dTEC values closed around a

Table 1
Number of Observations After Removing Erratic Data Points

Station/session	3 December	4 December	5 December	6 December	7 December
GGAO12M	1763	1279	1443	1247	1476
ISHIOKA	589	431	474	409	510
KOKEE12M	567	462	523	458	504
RAEGYEB	1183	303	587	5	630
WESTFORD	1735	1248	1401	98	1425
WETTZ13S	789	477	596	629	691

loop. The results indicated that there were some problems with the input data. After thorough investigations, we concluded the following:

1. The VGOS antennas receive and process signals in two orthogonal linear polarizations. These polarized signals follow independent signal paths once they are separated at the feed: they are amplified, filtered, and digitized independently and the digital signals are carried on separate fibers. As a result, there is typically a small delay between the two senses of polarization, which needs to be removed properly in post-processing. Small errors in determining and applying this delay, coupled with small errors due to source structure effects and errors in phase calibration may cause a phase curvature across frequency that is mistakenly lumped into a dTEC contribution.
2. Some of the radio sources (e.g., 0552 + 398) have large structure effects when observed on the VGOS baselines. They are spatially extended; some of them have two-point structures and the others have multiple-point structures (e.g., Xu et al., 2021). As it can be seen in Charlot (1990) the phase curvature will be affected by this error source and according to Equation 3, dTEC values will be changed as well.
3. The ionosphere is not always well-determined in the fringe fitting process. Due to the effects noted above, there can be multiple local maxima in the fringe amplitude near the "true" value of the dTEC. Sometimes these nearby maxima are larger than the correct peak and are thus chosen by fourfit.
4. Some of the signals (135 observations among 1180 observations) had poor SNR (signal-to-noise ratio). The data pipeline did not filter upon a threshold for SNR value, whereas all of the signals with the SNR less than 7 must be discarded (The high threshold of an SNR of 7 takes into consideration the "trials factor": since millions of individual points are searched in delay & rate space, detection needs to be 7 sigmas or more to be significant. This threshold only works for VGOS observations, while in the case of legacy VLBI, thresholds for X- and S-bands are typically higher). A least squares estimator has been used to derive the VTEC values from the dTEC data. Due to their potential strong effect on the solution, it was important to eliminate "blunder" points before fitting.
5. 5.The most significant error was found (by one of the authors, Roger Cappallo, who is also a principal author of fourfit) in the sign of the dTEC value reported by fourfit. Essentially, the value reported had an inverted sign due to an incorrect implicit ordering of the stations comprising the baseline. Since dTEC is in some sense a "nuisance parameter" to fourfit, a program that is primarily concerned with providing the best estimate of group delay, all dTEC values reported by fourfit have inadvertently had the opposite baseline difference sense from the other parameters. Within fourfit the code used the differenced value of dTEC with a compensating sign change so that there was no adverse effect on the geodetic observables; only the value of dTEC in the output data files had the unexpected sign.

Based on the problems noted above, the analysis code was modified. After flipping the signs of dTEC to solve the fifth problem, filtering out points having dTEC misclosures with a magnitude of more than 1 TECU to overcome first to third error sources, and removing observations with low SNR for the fourth mentioned problem, the data were reprocessed. The mapping function defined in Equation 7 is dependent on the zenith angle, that is, we have more VTEC in higher zenith angles. This introduces higher error in consequence, as the term w^k which defines the contribution of mapping function into parameters uncertainty, has the same relation with zenith angle. Therefore, in this study we removed the observations whose zenith angle was higher than 80°.

Table 1 shows the number of useful observations made in each station during the CONT17 Campaign. The number of observations during 4 and 6 December (4200 and 4262, respectively) is less than other sessions

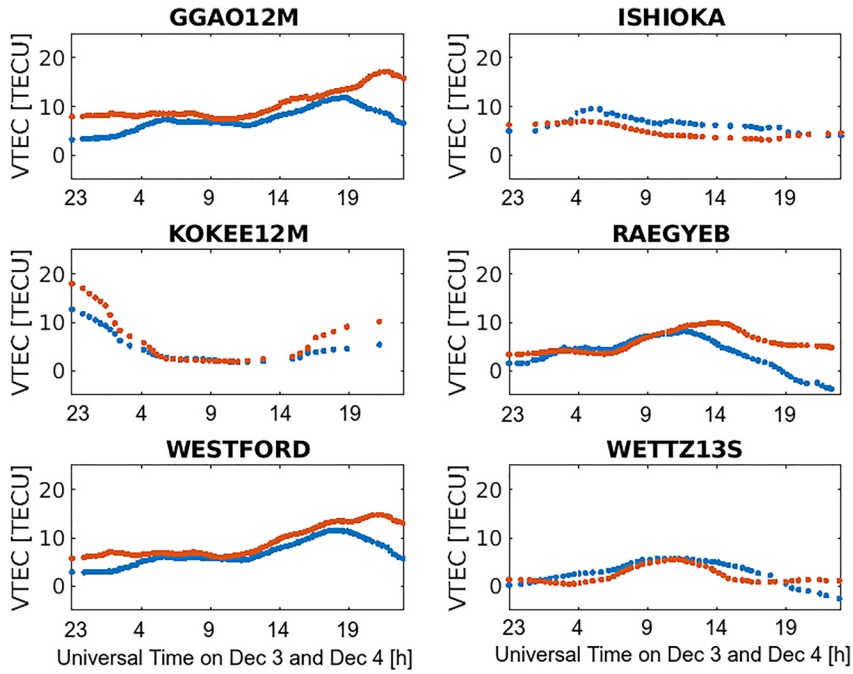

Figure 3. Comparison of vertical total electron content time series between VLBI global observing system (in blue) and global navigation satellite system (in red) for 3 December session (that continues until 23:00 UT of 4 December).

(e.g., 6626 observations on 3 December), due to the lack of observations from the RAEGYEB and WESTFORD stations. According to the information in log-files of these sessions, WESTFORD had difficulty slewing to sources on 6 December, which led to fewer observations. Also, during this time, RAEGYEB encountered pointing and instrumental stability problems, which reduced the antenna's sensitivity to observe sources. The pointing issue of RAEGYEB continued from the second day to the last day of the campaign; thus, as can be seen in Table 1, the number of observations in this station has been reduced in these days.

In all of the sessions, the number of observations in ISHIOKA and KOKEE12M is less than in others. This can be related to the geometry of the network. Based on Figure 2, KOKEE12M and ISHIOKA are located far east in latitude compared to four other stations. Moreover, WETTZ13S and KOKEE12M participated in the so-called Intensive sessions and were allowed to leave the campaign for an hour (Behrend et al., 2020). Intensive sessions are daily 1-hr sessions designed to estimate the dUT1 parameter (UT1-UTC). The baseline WETTZ13S-KOKEE12M is suitable for determining the dUT1 parameter because of its large east-west component (Corbin & Haas, 2019). During VGOS observation of the CONT17, these Intensive sessions were carried out, thus the smaller number of observations in these two stations can be explained by this reason.

The plots of the VTEC time series for 3 December 2017 are shown in Figure 3. The VTEC estimated from the first hour of observations in KOKEE12M (0–1 hr) has a discontinuity, most likely arising from a blunder point in the dTEC data. To get a more consistent fit, the observations involving KOKEE12M in this period were deleted.

The differences (GNSS-VGOS) and the standard deviations (σ) of estimated VTEC using GNSS and VGOS for the same day, are provided in Figure 4. The mean GNSS-VGOS difference for all stations is positive, which is consistent with the results of Dettmering et al. (2011), Hobiger et al. (2006), and Sekido et al. (2003) that GNSS-based VTEC is higher than VLBI-derived VTEC. For the whole CONT17 campaign, the difference GNSS-VGOS (in average) is at −2.1 TECU. For 3 December 2017, as seen in Figure 4, the standard deviation of estimating VTEC using VGOSranges from 0.3 TECU (WETTZ13S station, approximately at hour 30) to 2.6 TECU (ISHIOKA station, approximately at hour 30).

As mentioned in section 2-2, we did not use the non-negative constraint, because doing so would artificially place the blue line (VGOS VTEC) over the red line (GNSS VTEC) and consequently increase the difference between the two data sets. Thus, as can be seen in Figure 3, some points unexpectedly lie below zero. This is of

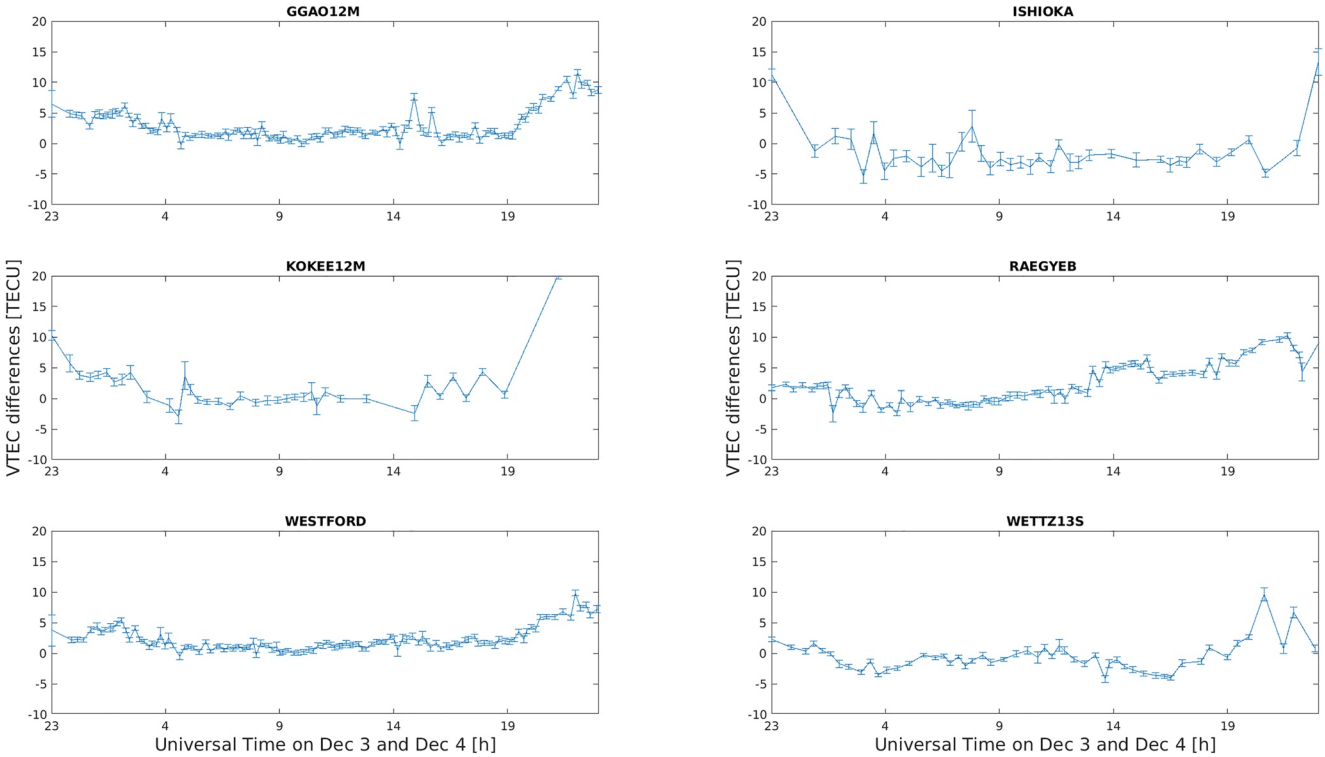

Figure 4. Differences (in the sense GNSS-VGOS) with 1σ error bars from the vertical total electron content estimations using VGOS for each station for 3 December session (that continues until 23:00 UT of 4 December).

course non-physical, as the VTEC cannot take negative values. This disagreement can be due to several reasons. The phasecal at the RAEGYEB site was erratic, and in the post-processing, a manual phase correction was made after the 12th hour of the observations, the point at which the divergence from GNSS VTEC starts in RAEGYEB (at hour 11th of 4 December). WETTZ13S experiences the same effect, but for a different reason, which is not understood, but may be related to unnoticed, and hence unfiltered, raw data points. Near the 21st hour of the time series, all of the stations start to diverge from the GNSS VTEC time series. This is because the negative values of RAEGYEB, due to the manual phasecal, that start at the same time and affect other stations as well.

To be able to derive one statistic for each session from the differences GNSS-VGOS per points in time, we formed the root mean square (RMS) of the differences between the individual VTECs at the same times with the equation below:

$$\mathrm{RMS} = \sqrt{\frac{\sum_{i=1}^{n}\left(\mathrm{VTEC}_i^{\mathrm{GNSS}} - \mathrm{VTEC}_i^{\mathrm{VGOS}}\right)^2}{n-1}} \tag{13}$$

where n is the number of VTEC estimates during one session. Equation 13 also removes the trend of the data from the RMS calculation. Table 2 shows the RMSof VTEC differences between VGOS and the GNSS for all of the sessions during CONT17, as well as the overall agreement between GNSS and VGOS for each day and each station. The RMS of differences between GNSS-VGOS ranges from 1.1 on 6 December for WESTFORD to 5.8 on 5 December for KOKEE12M. KOKEE12M has the highest overall RMS (4.1 TECU) as it is located near to equator. Thus, it experiences more fluctuation in ionosphere and appears to have a large difference from the GNSS data. The second worst station in comparison is RAEGYEB, as it has the greatest number of observations with an insufficient SNR. In all of the sessions, the best fit can be achieved for the WESTFORD, with the RMS of 1.5 TECU. Among the sessions of the CONT17 campaign, 6 December has the best fit with GNSS VTEC and the highest RMS has occurred in the 4 December session.

Using this algorithm, four other sessions observed during the CONT17 campaign were also processed; the results were consistent with the results of the first day. For the sake of brevity, Figures 5 and 6 show the VTEC time

Table 2
RMS of Vertical Total Electron Content Differences (Global Navigation Satellite System-VLBI Global Observing System) per Station for all of the Sessions

Station\session	RMS for 3 December (TECU)	RMS for 4 December (TECU)	RMS for 5 December (TECU)	RMS for 6 December (TECU)	RMS for 7 December (TECU)	Overall RMS for each station (TECU)
GGAO12M	2.20	2.35	1.80	1.36	1.46	1.83
ISHIOKA	2.33	3.17	1.71	3.01	3.36	2.71
KOKEE12M	3.52	4.03	5.84	3.46	3.80	4.13
RAEGYEB	4.13	3.39	3.96	3.11	3.56	3.63
WESTFORD	1.74	1.94	1.67	1.13	1.06	1.50
WETTZ13S	1.89	3.30	1.65	1.73	2.19	2.15
Overall RMS for each day (TECU)	2.64	3.03	2.77	2.30	2.57	

series extracted from VGOS observations during the 5 and 7 December sessions. Unlike the first day, the negative values for VTEC and the divergence starting from the 12th hour, are not seen in the results of other days including 5 and 7 December, as the problem with phasecal in RAEGYEB was resolved for the consequent days.

Another set of parameters we estimate is the time series representing the latitude gradient. For comparison, the time series of latitude gradient obtained from GIM data (the red curve) and the estimated gradient time series (the blue curve) for 3 December 2017 are shown in Figure 7. Consideration of Figure 7 suggests that the variation of latitude gradients is sensible. Our analysis spans 24 hr and it seemed that considering a single parameter for the whole span, such as that used in the original station-dependent model, is not a good solution, given the fluctuation of this parameter. Our estimated gradients are largely consistent with GIM data, and their differences are mostly in the order of a few tens of percent of the effect. As seen in Figure 8, where we show the differences and the standard deviations of estimation of these parameters using VGOS and GIM for 3 December 2017, ISHIOKA has the largest uncertainty of latitude gradient estimation using VGOS (approximately −2 TECU/deg of uncertainty). KOKEE12M has the greatest disagreement compared to GIM results (in the worst case, a difference of −1.5

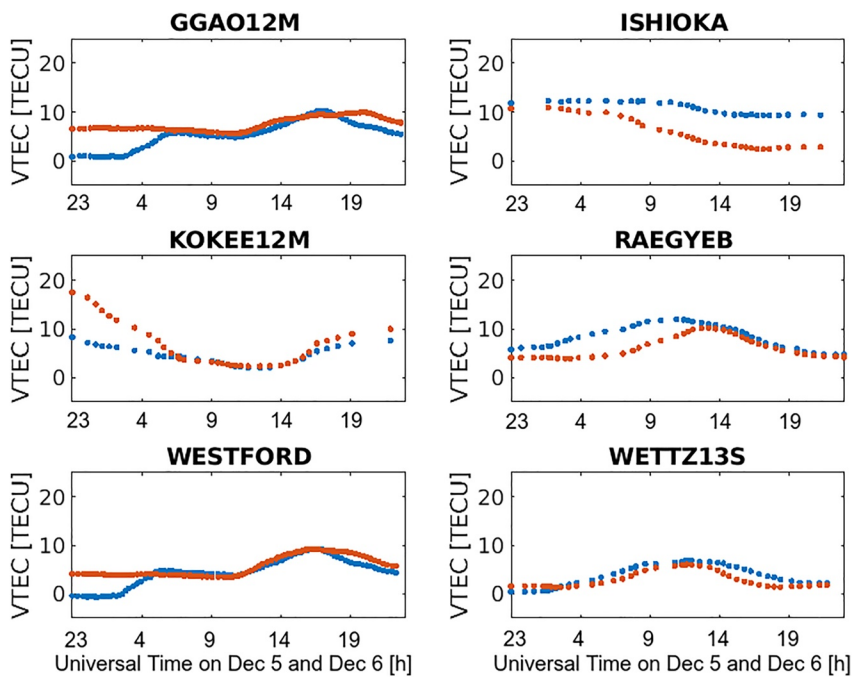

Figure 5. Comparison of vertical total electron content time series between VLBI global observing system (in blue) and GNSS (in red) for 5 December session (that continues until 23:00 UT of 6 December).

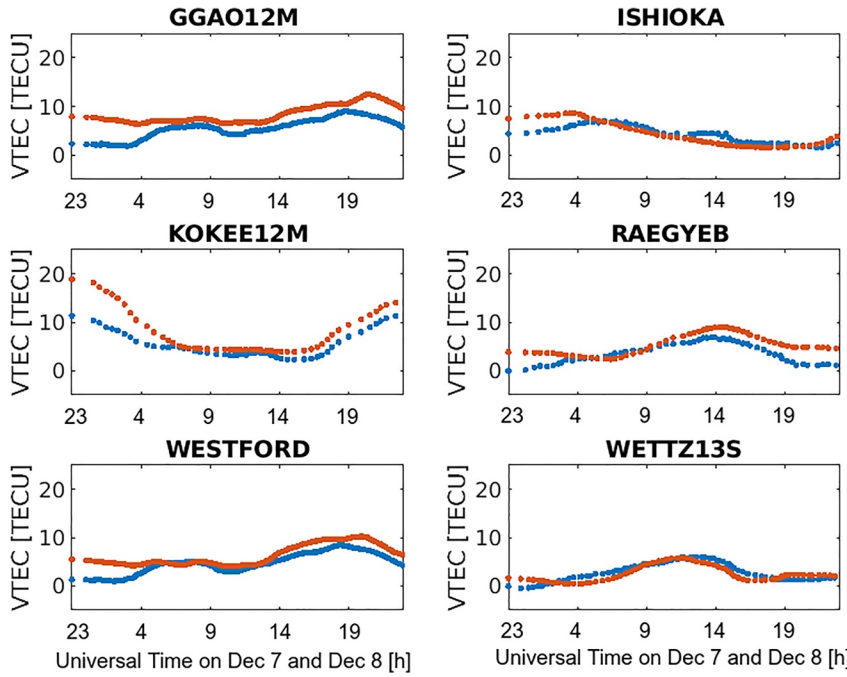

Figure 6. Comparison of vertical total electron content time series between VLBI global observing system (in blue) and global navigation satellite system (in red) for 7 December session (that continues until 23:00 UT of 8 December).

TECU). This can be attributed to the fact that this station has the lowest latitude among stations involved in this campaign, and thus experiences a TEC that is both larger and more variable.

The estimation accuracy of VTEC using GNSS can affect the comparison. Therefore, we compared the accuracy of each of the two methods for the whole VGOS sessions of CONT17 in Figure 9. The standard deviation of esti-

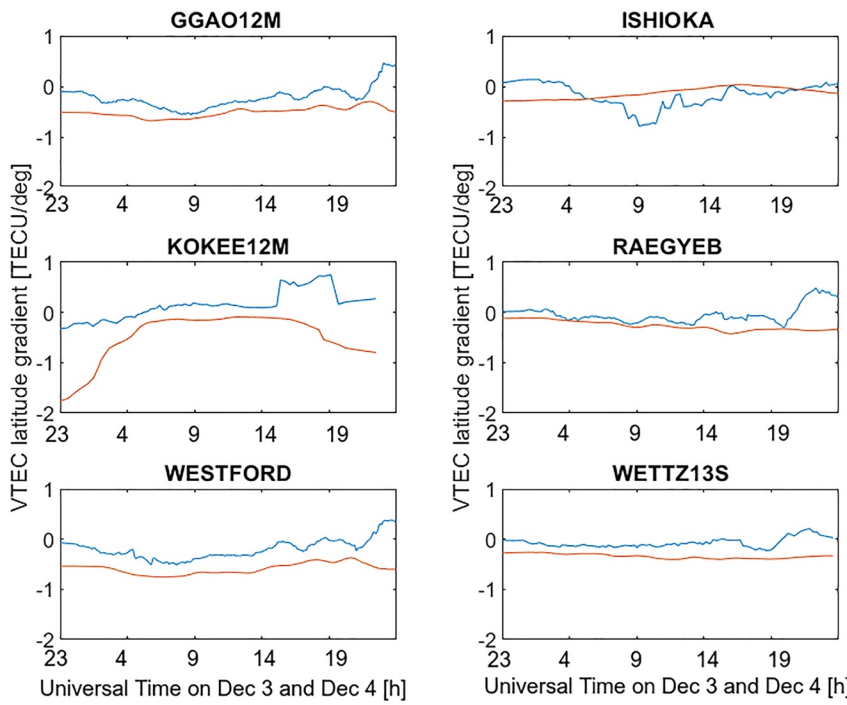

Figure 7. Time series of latitude gradients extracted from VLBI global observing system (blue line) versus the latitude gradients based on GIM (red line) for 3 December session (that continues until 23:00 UT of 4 December).

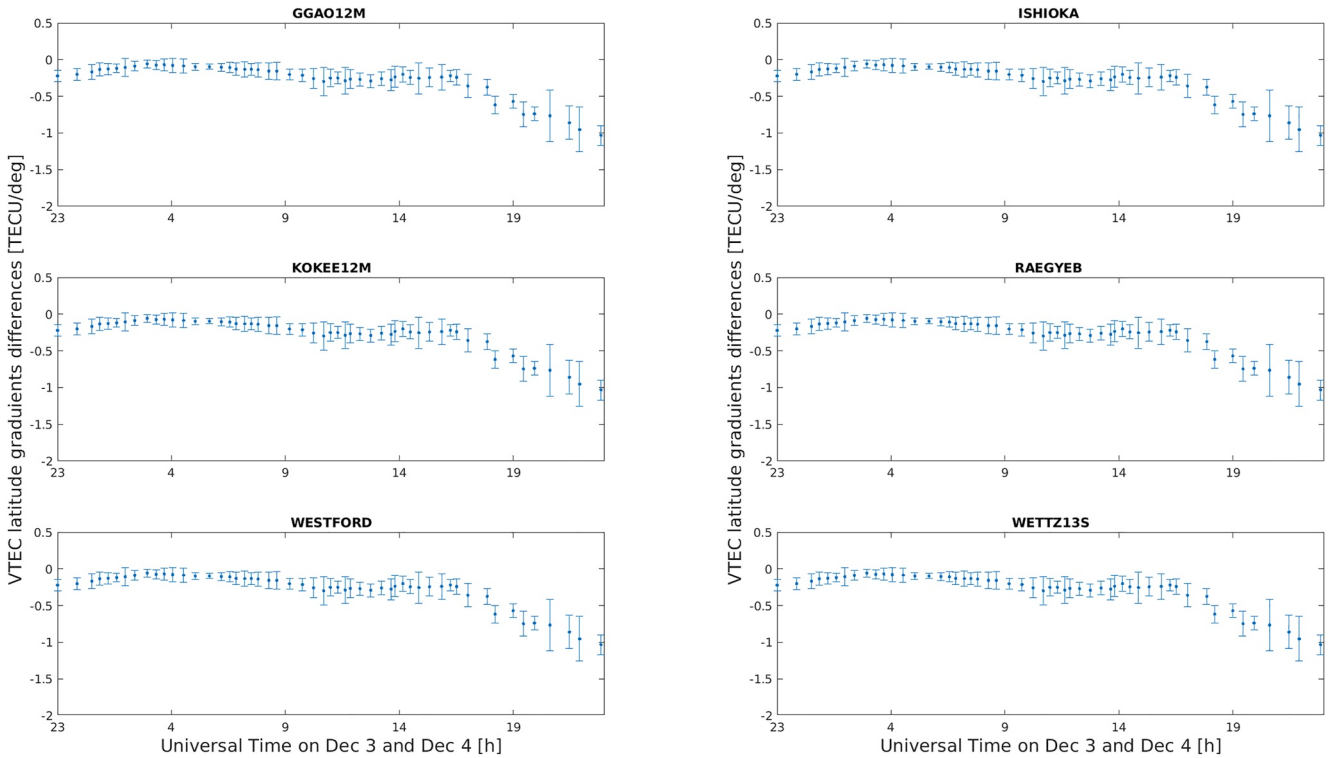

Figure 8. Differences (in the sense GIM-VGOS) with 1σ error bars from the latitude gradient estimations using VGOS for each station for 3 December session (that continues until 23:00 UT of 4 December).

mated VTEC using VGOS data is calculated through the least-square adjustment (Equation 12) and the standard deviation of GNSS VTEC is obtained from Gopi software. As seen in this figure, the standard deviation of VTEC estimations appears to be lower than that of the GNSS; specifically, as seen in the right plot of Figure 9, the average standard deviation of VGOS is 0.7, while the average standard deviation of GNSS is 1.8, which indicates that the accuracy of VTEC estimation using VGOS dTEC is within the error interval of GNSS and the agreement between two systems is good. Among all sessions, 4 December has the largest standard deviation both in VGOS and GNSS.

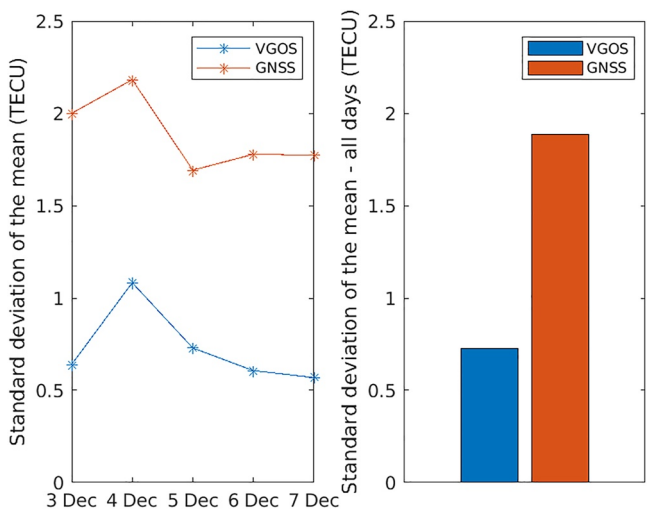

Figure 9. Comparison of vertical total electron content (VTEC) estimation using the two systems; the left plot shows the daily standard deviation of the mean for VTEC estimated from VLBI global observing system (VGOS) and global navigation satellite system (GNSS) for each session of the CONT17 and the right plot shows the standard deviation of the mean for all days for VTEC estimated from GNSS and VGOS during the CONT17.

Figure 10 compares the station-wise standard deviation of estimating VTEC using the two methods for the 3 December session. As seen in this figure, only in ISHIOKA the standard deviation of estimation of VTEC using VGOS is higher than that of GNSS. This station also had the highest standard deviation of estimation of latitude gradients. The reason for this station having a large uncertainty is not known, but can be understood in further studies.

5. Summary and Conclusion

In this paper, we tried a station-dependent model on dTEC data to construct the time series of VTEC as well as the ionospheric latitude gradient above each station involved in the CONT17 campaign. All dTEC observations in all 24-hr spans of VGOS data were processed and the VTEC values were extracted and compared with GNSS VTEC. The dTEC data used in this investigation are parameters calculated by the fourfit program, with a formal error of 0.04 TECU. The method used in this research is inspired by the work of Hobiger et al. (2006), which was designed for group delay observations of S/X VLBI. Since this was the first time this method was applied to

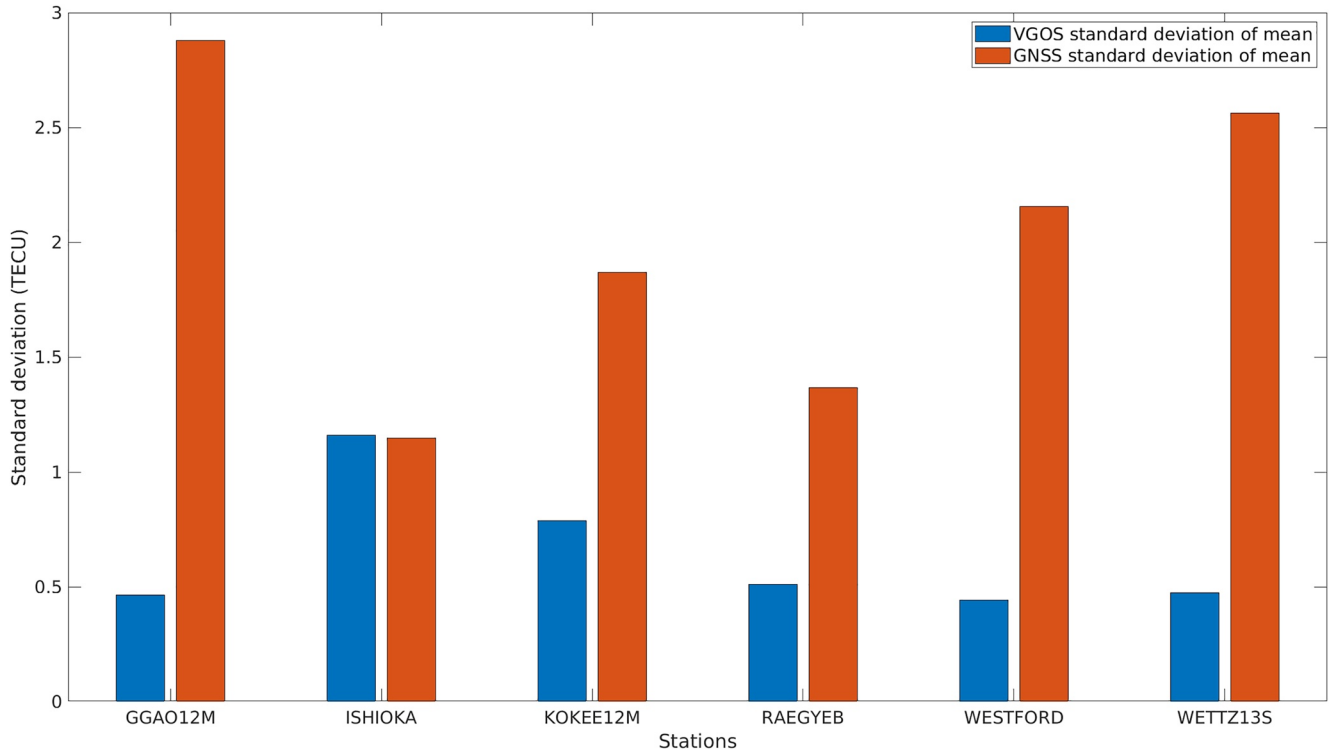

Figure 10. Comparison of vertical total electron content estimation standard deviation using the two systems for each station of 3 December 2017 session.

observations of the VGOS broadband system, many unexpected challenges arose, but ultimately the experience was successful. Even without comparison to the GNSS VTEC, the VTEC time series for the 3 December session displayed in Figure 3 are reasonable in general, because their peaks appear shortly after local noon (in which one sees the maximum solar activity and the largest TEC), for example, 23 UT of 3 December at KOKEE12M is 13 hr and it corresponds to the maximum value in TEC.

The average standard deviation of VTEC estimations from VGOS data during all of the CONT17 sessions is 0.7 TECU, which is within the range of GNSS standard deviation of estimates (on average 1.8 TECU). The average GNSS-VGOS difference during all sessions is positive (+2.1 TECU) which is consistent with the related studies that compared VLBI VTEC with GNSS VTEC. The RMS between VGOS-derived VTEC and GNSS-derived VTEC ranges from 1.1 to 5.8 TECU and on average is 3.4 TECU. Unsurprisingly, the KOKEE12M station, which lies closest to the equator, experienced the greatest fluctuation in ionosphere activity and consequently had the worst agreement with GNSS VTEC during the whole campaign (an RMS of 4.1 TECU). Among all stations that participated in VGOS sessions of CONT17, the WESTFORD station had the best agreement with GNSS VTEC, with an overall RMS of 1.5 TECU. Among all days of the CONT17 campaign, 4 December had the worst agreement with GIM-based VTEC (3.0 TECU), and 6 December had the best fit (2.3 TECU).

Another set of estimates was the time series of latitude gradient of the ionosphere, which was compared to that of GIM-based values. The RMS of the latitude gradients gets larger at ISHIOKA, while KOKEE12M has the worst agreement with GIM in the determination of latitude gradient. As expected, the KOKEE12M station also showed the worst agreement in the comparison to latitude gradient of GIM in all sessions. One contributing factor might be the larger GIM error in oceanic zones. In addition, the VLBI observations sample the ionosphere at a given point in time and a specific direction, which the smoothed (in time and space) GIM model cannot predict.

From the comparison of the first session results we saw that almost in all of the stations the standard deviation of VTEC estimates using VGOS data were lower than the standard deviation of GNSS VTEC. That does not necessarily mean that our estimations are better than GNSS. Nevertheless, one benefit of the current study is to

act as an independent check of the validity of the GNSS data, which has very different signal sources, geometries, and processing methods.

Acknowledgments
This study is based upon work done by the first author as a part of the requirements of an MSc degree at K. N. Toosi University of Technology. The revision of this manuscript has been done during the first author's presence in University of Helsinki as a PhD student funded by the academy of Finland. We also give credit to Dr. Sigrid Boehm, the head of the support team of VieVS software and express our appreciation to other colleagues at the MIT Haystack Observatory, namely, Anthea Coster, Mike Titus, and Geoffrey Crew, and from NVI Incorporated, John Gipson. We are grateful to all parties that contributed to the success of the CONT17 campaign, in particular to the IVS Coordinating Center at NASA Goddard Space Flight Center (GSFC) for taking the bulk of the organizational load, to the GSFC VLBI group for preparing the legacy S/X observing schedules and MIT Haystack Observatory for the VGOS observing schedules, to the IVS observing stations at Badary and Zelenchukskaya (both Institute for Applied Astronomy, IAA, St. Petersburg, Russia), Fortaleza (Rádio Observatório Espacial do Nordeste, ROEN; Center of Radio Astronomy and Astrophysics, Engineering School, Mackenzie Presbyterian University, Sao Paulo and Brazilian Instituto Nacional de Pesquisas Espaciais, INPE, Brazil), GGAO (MIT Haystack Observatory and NASA GSFC, USA), Hartebeesthoek (Hartebeesthoek Radio Astronomy Observatory, National Research Foundation, South Africa), the AuScope stations of Hobart, Katherine, and Yarragadee (Geoscience Australia, University of Tasmania), Ishioka (Geospatial Information Authority of Japan), Kashima (National Institute of Information and Communications Technology, Japan), Kokee Park (U.S. Naval Observatory and NASA GSFC, USA), Matera (Agencia Spatiale Italiana, Italy), Medicina (Istituto di Radioastronomia, Italy), Ny Ålesund (Kartverket, Norway), Onsala (Onsala Space Observatory, Chalmers University of Technology, Sweden), Seshan (Shanghai Astronomical Observatory, China), Warkworth (Auckland University of Technology, New Zealand), Westford (MIT Haystack Observatory), Wettzell (Bundesamt für Kartographie und Geodäsie and Technische Universität München, Germany), and Yebes (Instituto Geográfico Nacional, Spain) plus the Very Long Baseline Array (VLBA) stations of the Long Baseline Observatory (LBO) for carrying out the observations under the US Naval Observatory's time allocation, to the staff at the MPIfR/BKG correlator center, the VLBA correlator at Socorro, and the MIT Haystack Observatory correlator for performing the correlations and the fringe fitting of

Data Availability Statement

VGOS data during CONT17 are available from https://cddis.nasa.gov/archive/vlbi/ivsdata/vgosdb/2017/, GNSS data are accessible through https://cddis.nasa.gov/archive/gnss/data/daily/2017/, and https://data.unavco.org/archive/gnss/rinex3/obs/2017/, and GIM data are available from https://cddis.nasa.gov/archive/gnss/products/ionex/2017/. One needs to create an account in the Earth data system to access the data, which is simple and straightforward.

References

Barrett, J., Cappallo, R., Corey, B., Crew, G., Elosegui, P., Niell, A., et al. (2019). VGOS data processing manual. *MIT Haystack Observatory, Version, 1* (p. 32). Retrieved from https://www.haystack.mit.edu/wp-content/uploads/2020/07/docs_hops_000_vgos-data-processing.pdf

Behrend, D., Thomas, C., Gipson, J., Himwich, E., & Le Bail, K. (2020). On the organization of CONT17. *Journal of Geodesy*, *94*(10), 1–13. https://doi.org/10.1007/s00190-020-01436-x

Böhm, J., Böhm, S., Boisits, J., Girdiuk, A., Gruber, J., Hellerschmied, A., et al. (2018). Vienna VLBI and satellite software (VieVS) for geodesy and astrometry. *Publications of the Astronomical Society of the Pacific*, *130*(986), 044503. https://doi.org/10.1088/1538-3873/aaa22b

Böhm, J., & Schuh, H. (Eds.). (2013). *Atmospheric effects in space geodesy* (Vol. 5). Springer. https://doi.org/10.1007/978-3-642-36932-2

Cappallo, R. (2015). Covariance analysis of the simultaneous fit of group delay and dTEC in fourfit. In *Documentation of HOPS* (pp. 1–5). Retrieved from https://www.haystack.mit.edu/wp-content/uploads/2020/07/docs_hops_014_simul_ion_fit.pdf

Cappallo, R. (2016). Delay and phase calibration in VGOS post-processing. In *IVS 2016 General Meeting Proceedings* (pp. 61–64). Retrieved from https://ivscc.gsfc.nasa.gov/publications/gm2016/010_cappallo.pdf

Cappallo, R. (2017). FOURFIT user's manual. Retrieved from https://www.haystack.mit.edu/wp-content/uploads/2020/07/docs_hops_009_fourfit_users_manual.pdf

Charlot, P. (1990). Radio-source structure in astrometric and geodetic very long baseline interferometry. *The Astronomical Journal*, *99*, 1309–1326. https://doi.org/10.1086/115419

Corbin, A., & Haas, R. (2019). Scheduling of twin telescopes and the Impact on troposphere and UT1 estimation. In *Proceedings of the 24th European VLBI Group for Geodesy and Astrometry Working Meeting* (pp. 194–198). https://doi.org/10.7419/162.08.2019

Cotton, W. D. (1995). Fringe fitting. In J. A. Zensus, P. J. Diamond, & P. J. Napier (Eds.), *Very Long Baseline Interferometry and the VLBA-RAO Workshop No. 22*, *Astronomical Society of the Pacific Conference Series* (Vol. 82, p. 189). Retrieved from https://www.aspbooks.org/a/volumes/article_details/?paper_id=11109

Dettmering, D., Heinkelmann, R., & Schmidt, M. (2011). Systematic differences between VTEC obtained by different space-geodetic techniques during CONT08. *Journal of Geodesy*, *85*(7), 443–451. https://doi.org/10.1007/s00190-011-0473-z

Gipson, J. (2015). Practical uses of VGOSDB format. In *Proceedings of the 22nd European VLBI Group for Geodesy and Astrometry Working Meeting 18–21 May 2015 Ponta Delgada* (pp. 97–101). Retrieved from https://www.oan.es/raege/evga2015/EVGA2015_proceedings.pdf

Hawarey, M., Hobiger, T., & Schuh, H. (2005). Effects of the 2nd order ionospheric terms on VLBI measurements. *Geophysical Research Letters*, *32*(11), L11304. https://doi.org/10.1029/2005GL022729

Hobiger, T., Kondo, T., & Schuh, H. (2006). Very long baseline interferometry as a tool to probe the ionosphere. *Radio Science*, *41*(01), 1–10. https://doi.org/10.1029/2005RS003297

Hobiger, T., & Schuh, H. (2004). Modelling vertical total electron content from VLBI observations. In *International VLBI Service for Geodesy and Astrometry 2004 General Meeting Proceedings* (pp. 306–310). NASA/CP-2004-212255.Retrieved from https://ivscc.gsfc.nasa.gov/publications/gm2004/hobiger2.pdf

Hofmann-Wellenhof, B., Lichtenegger, H., & Collins, J. (2001). Applications of GPS. In *Global Positioning System* (pp. 319–343). Springer. Retrieved from https://link.springer.com/chapter/10.1007/978-3-7091-6199-9_12

Koch, K. R. (1997). *Parameter estimation and hypothesis testing in linear models*. Springer Science & Business Media. https://doi.org/10.1007/978-3-662-03976-2

Niell, A., Barrett, J., Burns, A., Cappallo, R., Corey, B., Derome, M., et al. (2018). Demonstration of a broadband very long baseline interferometer system: A new instrument for high-precision space geodesy. *Radio Science*, *53*(10), 1269–1291. https://doi.org/10.1029/2018RS006617

Nothnagel, A., Artz, T., Behrend, D., & Malkin, Z. (2017). International VLBI service for geodesy and astrometry. *Journal of Geodesy*, *91*(7), 711–721. https://doi.org/10.1007/s00190-016-0950-5

Petrachenko, B., Niell, A., Behrend, D., Corey, B., Böhm, J., Chralot, et al. (2009). *Design aspects of the VLBI2010 system, progress report of the IVS VLBI2010 Committee*. NASA. TM-2009-214180. Retrieved from https://ivscc.gsfc.nasa.gov/technology/vgos-docs/PR-V2C_090417.pdf

Rocken, C., Meertens, C., Stephens, B., Braun, J., VanHove, T., Perry, S., et al. (1995). *UNAVCO Academic Research Infrastructure (ARI) receiver and antenna test report*. University Corporation for Atmospheric Research/University NAVSTAR Consortium. Retrieved from https://www.unavco.org/projects/project-support/development-testing/publications/ari_test.pdf

Rogers, A. E. E. (1970). Very long baseline interferometry with large effective bandwidth for phase-delay measurements. *Radio Science*, *5*(10), 1239–1247. https://doi.org/10.1029/RS005i010p01239

Roma-Dollase, D., Hernández-Pajares, M., Krankowski, A., Kotulak, K., Ghoddousi-Fard, R., Yuan, Y., et al. (2018). Consistency of seven different GNSS global ionospheric mapping techniques during one solar cycle. *Journal of Geodesy*, *92*(6), 691–706. Retrieved from https://link.springer.com/article/10.1007/s00190-017-1088-9

Romero, I. (2020). The receiver independent exchange format version 3.05. Retrieved from https://files.igs.org/pub/data/format/rinex305.pdf

Schaer, S. (1999). *Mapping and predicting the Earth's ionosphere using the global positioning system, Ph.D. Dissertation*. Univ. Bern. Retrieved from http://ftp.aiub.unibe.ch/papers/ionodiss.pdf

Schaer, S., Gurtner, W., & Feltens, J. (1998). IONEX: The ionosphere map exchange format version 1. In *Proceedings of the IGS AC Workshop* (Vol. 9. p. 11). Retrieved from http://ftp.aiub.unibe.ch/ionex/draft/ionex11.pdf

the data, and to the IVS Data Centers at BKG (Leipzig, Germany), Observatoire de Paris (France), and NASA CDDIS (Greenbelt, MD, USA) for the central data holds.

Seemala, G. K. (2011). *GPS-TEC analysis application read me*. Institute for Scientific Research. Retrieved from https://drive.google.com/file/d/0BzKakBf8mqOZNTUxNTAxNTktZTEyNi00NmVjLTk5YjAtMTA1MjFjYTdlYTI5/view?usp=sharing%26resourcekey=0-drGUMZH-ud_mHaluuB2fHw

Seemala, G. K., & Valladares, C. E. (2011). Statistics of total electron content depletions observed over the South American continent for the year 2008. *Radio Science*, *46*(5), 1–14. https://doi.org/10.1029/2011RS004722

Sekido, M., Kondo, T., Kawai, E., & Imae, M. (2003). Evaluation of GPS-based ionospheric TEC map by comparing with VLBI data. *Radio Science*, *38*(4), 1069. https://doi.org/10.1029/2000rs002620

Xu, M. H., Savolainen, T., Zubko, N., Poutanen, M., Lunz, S., Schuh, H., & Wang, G. L. (2021). Imaging VGOS observations and investigating source structure effects. *Journal of Geophysical Research: Solid Earth*, *126*(4), e2020JB021238. https://doi.org/10.1029/2020JB021238